Crystal Structure and Elementary Physical Properties of La$_5$Cu$_{19}$P$_{12}$ and Ce$_5$Cu$_{19}$P$_{12}$

R. J. Cava, T. Siegrist, S. A. Carter, J. J. Krajewski, and W. F. Peck, Jr.

AT&T Bell Laboratories, Murray Hill, New Jersey 07974

and

H. W. Zandbergen

National Centre for Electron Microscopy, Technical University Delft, The Netherlands

DEDICATED TO THE MEMORY OF ALEXANDER F. WELLS

The syntheses of La$_5$Cu$_{19}$P$_{12}$ and Ce$_5$Cu$_{19}$P$_{12}$ are reported, as is the crystal structure of La$_5$Cu$_{19}$P$_{12}$, determined by single crystal X-ray diffraction. The compounds are found to be of the Sc$_5$Co$_{19}$P$_{12}$ structure type. Both new materials are metallic, with the resistivity of Ce$_5$Cu$_{19}$P$_{12}$ characteristic of heavy fermion behavior. The magnetic susceptibility of Ce$_5$Cu$_{19}$P$_{12}$ shows the signature of a crystal electric field (CEF) split 4f multiplet for Ce, with a high temperature effective moment of $P_{\text{eff}} = 1.71(2)$ μ_{B}/mole Ce. For La$_5$Cu$_{19}$P$_{12}$, no local moment is observed for copper. © 1996 Academic Press, Inc.

INTRODUCTION

A wide variety of structurally interesting intermetallic phosphide compounds are known. The physical properties of many of the more complex materials are largely uncharacterized. We have recently been exploring a new family of intermetallic superconductors based on Ni (1) and have been searching for new Cu based intermetallic compounds to look for possible analogies with copper oxide superconductors. Here we report the crystal structure and elementary physical properties of La$_5$Cu$_{19}$P$_{12}$, a hexagonal symmetry material of the Sc$_5$Co$_{19}$P$_{12}$-type (2) in which the Cu and P form a three-dimensional network and the La atoms occur in one-dimensional columns. We have also synthesized the Ce analog, Ce$_5$Cu$_{19}$P$_{12}$, to test its physical properties based on the fact that CeCu$_2$Si$_2$ is a well-known heavy electron mass superconductor. The physical property measurements show La$_5$Cu$_{19}$P$_{12}$ to be metallic with no local moment and that Ce$_5$Cu$_{19}$P$_{12}$ does indeed show characteristics of heavy fermions, although it is not superconducting above 1.8 K, with a magnetic ordering of the Ce moments at 7.5 K.

SYNTHESIS

Starting materials were high purity lanthanide (99.99%) metal shavings, coarse Cu powder, and lump red phosphorus (>99.99%). First, the lanthanide and copper metals were arc melted together under argon (3×). The phosphorus weighing and handling was performed in an N$_2$ purged drybox. The Ln–Cu alloys were ground to a powder, mixed with phosphorus in 0.75-g batches, pressed into 1/8-in. diameter pellets, and put into dense Al$_2$O$_3$ crucibles and then into evacuated quartz tubes. Samples were slowly heated to 900°C over a period of several days. They were annealed at 900°C until no free P was observed in the tubes after cooling to room temperature. Samples were then ground, repressed into pills, and reheated, following this procedure several times with annealing at a final temperature of 1100°C until the powder X-ray diffraction pattern showed them to be single phase. During one of the synthetic runs in our initial La–Cu–P exploratory syntheses, small prismatic crystals of the new phase grew on the pellets. One of these crystals was employed for the structure determination. Our attempts to synthesize Sm$_5$Cu$_{19}$P$_{12}$, by the same method to test for the stability of the phase for an intermediate size lanthanide, were not successful.

CRYSTAL STRUCTURE DETERMINATION

Intensity data for a small single crystal (0.05 × 0.05 × 0.25 mm) of La$_5$Cu$_{19}$P$_{12}$ were collected on a Nonius diffractometer with Mo$K\alpha$ radiation using the theta/two theta scan mode. The structure refinement was based on 652 unique reflections with intensities greater than 2.5σ, corrected for absorbtion; a total of 7171 reflections were

TABLE 1
Crystallographic Characterization of $La_5Cu_{19}P_{12}$

(a) Symmetry: hexagonal, space group $P\bar{6}2m$ (Noncentrosymmetric)
Cell Dimensions: $a_o = 12.7730(10)$, $c_o = 3.9876(3)$
Density, calculated: 6.413 g/cm^3

(b) Atomic parameters x, y, z, and $Biso^a$

	x	y	z	$Biso^b$
La 1	2/3	1/3	0	0.65(3)
La 2	0.19329(9)	0.19329	1/2	0.62(4)
Cu 1	0	0	0	0.84(12)
Cu 2	0.71219(21)	0.71219	1/2	0.98(10)
Cu 3	0.37827(20)	0.17247(22)	0	1.24(9)
Cu 4	0.63588(21)	0.11849(20)	1/2	1.23(9)
Cu 5	0.5492(4)	0.5492	0	6.5(3)
P 1	0.8232(5)	0.8232	0	0.62(18)
P 2	0.3702(5)	0.3702	0	0.87(19)
P 3	0.4796(4)	0.1724(4)	1/2	0.88(18)

(c) Table of $u(i, j)$ or U values $*100^{a,c}$

	$u_{11}(U)$	u_{22}	u_{33}	u_{12}
La1	0.92(4)	0.92	0.63(6)	0.46
La2	0.79(4)	0.79	0.66(5)	0.33(4)
Cu1	0.81(11)	0.81	1.59(22)	0.40
Cu2	1.04(9)	1.04	1.59(13)	0.47(11)
Cu3	1.08(9)	2.26(11)	1.25(9)	0.73(8)
Cu4	1.60(10)	1.24(9)	2.07(10)	0.90(8)
Cu5	3.55(17)	3.55	12.4(6)	−2.05(25)
P1	0.83(16)	0.83	0.86(24)	0.54(20)
P2	0.96(18)	0.96	1.01(24)	0.20(23)
P3	1.17(20)	0.90(16)	1.22(18)	0.48(15)

[a] e.s.d: values refer to the last digit printed.
[b] $Biso$ is the mean of the principal axes of the thermal ellipsoid.
[c] The thermal parameter (T) is of the form $T = 2\pi^2(h^2 \cdot u_{11} \cdot a^{*2} + 2hk \cdot u_{12} \cdot a^*b^* + \text{---})$.

averaged for the final data set. Unit cell dimensions were refined from 33 reflections with $50.00° \leq 2\Theta \leq 60.00°$. The structure was refined with the NRCVAX suite of programs. The final residual, $R_F (\Sigma (F_o - F_c)/\Sigma (F_o))$, was 0.026. The refined crystal structure and atomic coordinates are presented in Table 1. The calculated powder X-ray diffraction pattern for $La_5Cu_{19}P_{12}$ (Cu$K\alpha$ radiation) is presented in Table 2. Based on the information in Table 1, the powder X-ray diffraction pattern of $Ce_5Cu_{19}P_{12}$ could be fully indexed, with approximate unit cell parameters $a_o = 12.75$ Å, $c_o = 3.94$ Å.

For one of the copper atoms (Cu5) the large anisotropic thermal parameter along c (u_{33} in Table 1c) is characteristic of displacive disorder. This disorder is observed for many of the compounds of this structure type (3, 4) where it has been modeled by allowing the Cu5 position to split into four equivalent positions with $z \neq 0$. The disorder can represent either a true positional disorder or the presence of an ordered supercell with weak reflections not detected

in the X-ray diffraction experiment. To test for this possibility, $La_5Cu_{19}P_{12}$ was investigated by electron diffraction, which is very sensitive to weak supercell reflections, in a Phillips CM30ST electron microscope operating at 300 kV equipped with a side entry 25°/25° tilting stage. Inspection of a variety of diffraction zones including the $hk0$, $h0l$, and hhl zones did not reveal any reflections not indexed by the hexagonal 12.77 by 3.99 Å cell. The Cu5 atom can therefore be concluded to occupy one of each of its four possible sites per unit cell in a disordered manner from one cell to the next. When refined in the "split atom" model, the Cu5 position is $x = 0.5377(5)$, $y = 0.5579(5)$, $z = 0.065(1)$, with occupancy 0.25; the R value is not different from the anisotropic vibration model presented in Table 1.

TABLE 2
Calculated Powder X-Ray Diffraction Pattern for $La_5Cu_{19}P_{12}$ (Cu$K\alpha$)

| h	k	l	2Θ	D space	Intensity
1	1	0	13.86	6.384	1
2	0	0	16.02	5.528	2
2	1	0	21.24	4.179	5
1	0	1	23.70	3.751	5
3	0	0	24.12	3.687	1
1	1	1	26.34	3.381	13
2	0	1	27.58	3.231	1
2	2	0	27.92	3.193	9
3	1	0	29.08	3.068	9
2	1	1	30.98	2.8841	8
3	0	1	33.08	2.7057	9
3	2	0	35.34	2.5376	7
2	2	1	36.00	2.4926	100
3	1	1	36.94	2.4313	24
4	1	0	37.22	2.4137	24
4	0	1	39.64	2.2717	5
5	0	0	40.76	2.2118	6
3	2	1	42.18	2.1406	2
3	3	0	42.42	2.1290	7
4	2	0	43.24	2.0905	3
4	1	1	43.80	2.0651	8
0	0	2	45.46	1.9935	23
5	0	1	46.94	1.9340	3
3	3	1	48.44	1.8776	8
6	0	0	49.40	1.8433	14
4	3	0	50.12	1.8185	2
2	1	2	50.68	1.7997	1
5	1	1	51.34	1.7781	2
2	2	2	54.20	1.6909	2
3	1	2	54.88	1.6715	3
4	3	1	55.50	1.6543	8
5	2	1	56.84	1.6184	4
5	3	0	58.34	1.5803	2
3	2	2	58.86	1.5676	2
6	1	1	59.44	1.5537	4
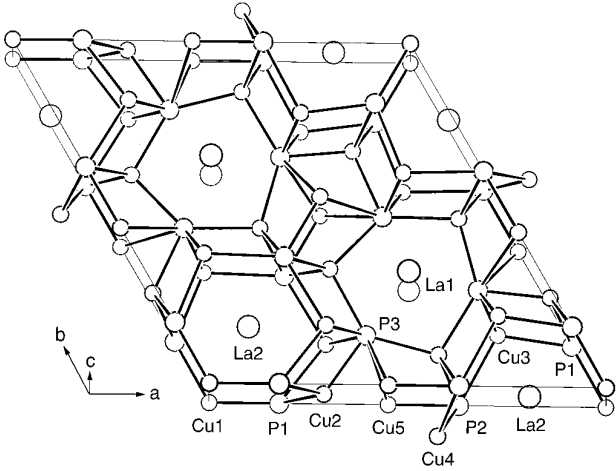
FIG. 1. The crystal structure of La$_5$Cu$_{19}$P$_{12}$, atoms identified as marked, large, medium, and small circles as lanthanum, phosphorus, and copper, respectively. Copper–phosphorous bonds shown as bold lines.

FIG. 2. The temperature-dependent resistivity of polycrystalline La$_5$Cu$_{19}$P$_{12}$. The inset shows the T^2 dependence of the resistivity for temperatures less than 70 K.

The crystal structure is shown in Fig. 1. The illustration emphasizes the three-dimensional Cu–P array by highlighting the Cu–P chemical bonds. The distorted hexagonal tunnels which accommodate the lanthanides are also apparent, running along the c axis. Note that the triangular planar array of lanthanide atoms has the potential for geometric frustration of the magnetic ordering of the lanthanide magnetic moments, although that frustration apparently does not occur for Ce$_5$Cu$_{19}$P$_{12}$, which shows magnetic ordering at 7.5 K.

The present compounds are the first of this structure type which are based on Cu. The structure type occurs extensively for Co, for Ln_5Co$_{19}$P$_{12}$, Ln = Gd–Lu, Y, Sc, and Zr (3, 4), and for Ru, for Ln_5Ru$_{19}$P$_{12}$ (5). It has also been observed for one Ni based compound, Ho$_5$Ni$_{19}$P$_{12}$ (6). The present materials extend the range of the phase beyond the group eight transition metals, and show that it is stable for a significant range of electron count.

The coordination numbers of the lanthanum atoms are quite high, 15 for La1 and 16 for La2. The lanthanides are located in channels formed by hexagonal prisms, with three or four sides capped by additional copper atoms. The three-dimensional copper-phosphorus framework shows three different environments for the copper atoms, which all have phosphorus as nearest neighbors: (I) trigonal, as for Cu1 (Cu–P: 2.26 Å), (II) distorted tetrahedral, as for Cu2, Cu3, and Cu4 (Cu–P: 2.34 to 2.58 Å), and (III) ''linear'', as for Cu5 (Cu–P: 2.29 Å). The contacts of copper to other copper atoms are quite short, ranging from 2.62 to 2.93 Å. For the anisotropic model refinement Cu5 is a special case, with only one phosphorus at 2.29 Å, but four more at 2.85 Å, a distance approximately equal to its copper–copper contacts which range from 2.78 to 2.88 Å. When refined as a displaced atom, Cu5 has two near P neighbors, P2 at
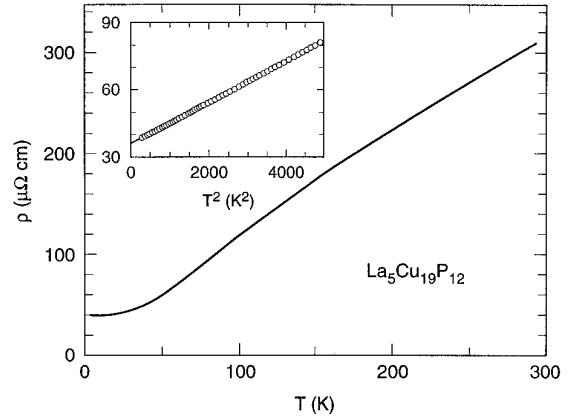
2.309(8) and P3 at 2.516(9) Å, two further P3 neighbors at 2.86(1) and 2.896(8) Å, and three copper–copper contacts of 2.590(5) (Cu4), 2.640(6) (Cu3), and 2.727(6) (Cu2).

PHYSICAL PROPERTIES

Figures 2 and 3 present the temperature-dependent resistivity and magnetic susceptibility for La$_5$Cu$_{19}$P$_{12}$, measured on polycrystalline samples. La$_5$Cu$_{19}$P$_{12}$ is a good metal with a resistivity ratio of approximately 8 ($\rho_{300}/\rho_{4.2}$) and a residual resistivity of 40 $\mu\,\Omega$-cm. Due to the granular nature of the sample, some of the residual resistivity may be due to the presence of grain boundaries. The inset to Fig. 2 shows that the low-temperature resistivity (10–70 K) follows good T^2 behavior, as expected for a resistivity dominated by electron–electron interactions. Figure 3 shows that the magnetic susceptibility of La$_5$Cu$_{19}$P$_{12}$ is pre-
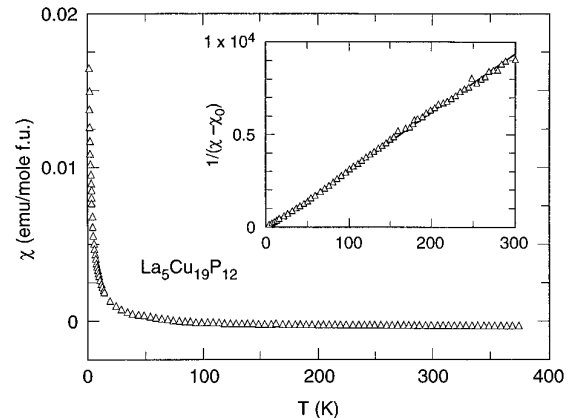

FIG. 3. The temperature-dependent magnetic susceptibility of La$_5$Cu$_{19}$P$_{12}$. Inset: fit of the low-temperature data to the Curie–Weiss law after subtraction of χ_o.

TABLE 3
Interatomic Distances in $La_5Cu_{19}P_{12}$

La1	–Cu3	3.197(6)	3×	La2	–Cu1	3.173(2)	2×
	–Cu4	3.253(5)	6×		–Cu2	3.246(8)	2×
	–P3	3.000(8)	6×		–Cu3	3.203(2)	4×
					–Cu4	3.218(4)	2×
					–P1	3.098(12)	4×
					–P2	3.014(5)	2×
Cu1	–P1	2.259(12)	3×	Cu2	–P1	2.446(4)	2×
					–P2	2.336(10)	2×
Cu3	–P1	2.409(3)			–Cu3	2.760(5)	4×
	–P2	2.579(4)			–Cu5	2.883(4)	2×
	–P3	2.378(3)	2×	Cu4	–P2	2.481(10)	2×
	–Cu2	2.760(5)	2×		–P3	2.415(6)	
	–Cu4	2.912(3)	2×		–P3	2.430(4)	
	–Cu5	2.785(13)			–Cu3	2.912(3)	2×
					–Cu4	2.622(6)	
Cu5	–P2	2.285(8)			–Cu5	2.877(5)	2×
	–P3	2.855(9)	4×				
	–Cu2	2.883(4)	2×				
	–Cu3	2.785(13)	2×				
	–Cu4	2.877(5)	4×				

FIG. 5. Temperature-dependent resistivity of a polycrystalline sample of $Ce_5Cu_{19}P_{12}$. Inset: low-temperature data.

dominantly independent of temperature. The temperature independent component χ_o is found to be diamagnetic and relatively small ($\sim 5.2 \times 10^{-4}$ emu/mole f.u.). The insert shows that after subtraction of χ_o the remainder can be fit to Curie law behavior with the Curie constant $C = 3.4 \times 10^{-2}$ emu K/mole f.u., which assuming $g = 2$, yields an effective moment of 0.1 μ_B per formula unit. This could be due to the presence of small levels ($<0.5\%$) of Cu^{2+} impurities in the sample. Overall, the magnetic susceptibility shows that the Cu is not in a magnetic state; i.e., its d levels are completely or nearly completely filled.

The magnetic susceptibility and resistivity of $Ce_5Cu_{19}P_{12}$ are both quite different from those of the La analog, as shown in Figs. 4 and 5. The magnetic susceptibility (Fig. 4) shows the exp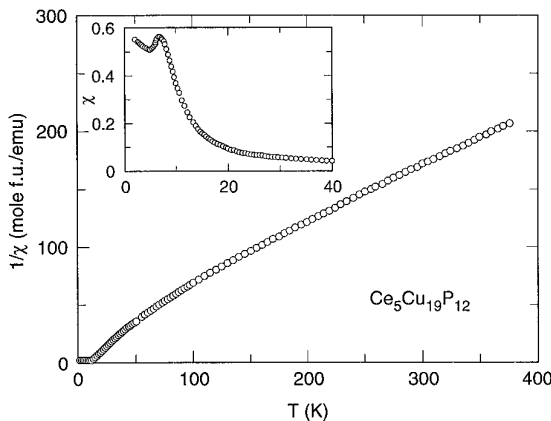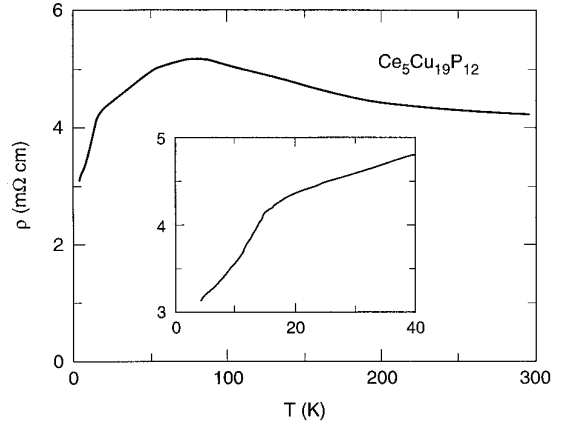ected behavior for the Ce^{3+} $4f$ multiplet split by the crystal-electric field (CEF). A fit to the high-temperature data (120/400 K) reveals a Ce moment of 1.71(2) μ_B, compared to the expected Ce^{3+} moment of 2.54 μ_B. The lower value suggests that the angular momentum of the trivalent cerium is quenched. The temperature independent part of χ is paramagnetic and small ($\chi_0 \sim 5 \times 10^{-4}$ emu/mole f.u.) indicating only weak enhancement by electron–electron interactions. The curvature in $1/\chi$ vs T at low temperatures is due to the CEF. The magnetic data (inset, Fig. 4) suggest a magnetic ordering of the Ce moments between 7 and 8 K. (We note that CeP orders antiferromagnetically at 8.5 K. Further study may be necessary to determine whether the apparent magnetic ordering observed is due to the presence of a very small amount of CeP impurity phase.) The resistivity of a polycrystalline sample of $Ce_5Cu_{19}P_{12}$ is shown in Fig. 5. Its resistivity is approximately an order of magnitude larger than that of $La_5Cu_{19}P_{12}$ and shows a temperature dependence characteristic of single-ion Kondo metals, like $CeAl_3$. There is no apparent signature of the magnetic ordering in the resistivity which shows a down-turn at low temperatures, perhaps associated with coherent electron effects.

CONCLUSIONS

We have characterized the crystal structure and elementary physical properties of $La_5Cu_{19}P_{12}$ and $Ce_5Cu_{19}P_{12}$; the latter may be worth further study at lower temperatures to look for superconductivity. It is interesting that when based on copper, the $Ln_5T_5P_{12}$ structure type exists for the large rare earths La and Ce, whereas when based on cobalt the stability is limited to the smaller rare earths. Although we were not successful in synthesizing $Sm_5Cu_{19}P_{12}$ by our method we did not extensively explore the synthesis of other possible $Ln_5Cu_{19}P_{12}$ compounds. Although the chem-

FIG. 4. Inverse magnetic susceptibility, $1/\chi$, vs temperature for $Ce_5Cu_{19}P_{12}$. Inset χ vs T in the vicinity of the apparent magnetic ordering.

istry and crystal structures of intermetallic compounds have been widely studied, continued exploration of the physical properties of more complex materials will be a fruitful area of basic and applied research in the future.

REFERENCES

1. R. J. Cava, H. Takagi, H. W. Zandbergen, J. J. Krajewski, W. F. Peck, Jr., T. Siegrist, B. Batlogg, R. B. van Dover, R. J. Felder, K. Mizuhashi, J. O. Lee, H. Eisaki, and S. Uchida, *Nature* **367,** 252 (1994).

2. W. Jeitschko and E. J. Reinhold, *Z. Naturforsch. B* **40,** 900 (1985).

3. V. Ghetta, P. Chaudouet, R. Madar, J. P. Senateur, and B. Lambert-Andron, *J. Less. Common Met.* **120,** 197 (1986).

4. U. Jakubowski-Ripke and W. Jeitschko, *J. Less Common Met.* **136,** 261 (1988).

5. V. Ghetta, P. Chaudouet, R. Madar, J. P. Senateur, and B. Lambert-Andron, *J. Less. Common Met.* **146,** 299 (1989).

6. J. Y. Pivan, R. Guerin, and M. Sergent, *Inorg. Chim. Acta.* **109,** 221 (1985).